

Biological Lasers for Biomedical Applications

Yu-Cheng Chen* and Xudong Fan*

A biolaser utilizes biological materials as part of its gain medium and/or part of its cavity. It can also be a micro- or nanosized laser embedded/integrated within biological materials. The biolaser employs lasing emission rather than regular fluorescence as the sensing signal and therefore has a number of unique advantages that can be explored for broad applications in biosensing, labeling, tracking, contrast agent development, and bioimaging. This article reports on the progress in biolasers with focus on the work done in the past five years. In the end, the possible future directions of the biolaser are discussed.

1. Introduction

Biolaser or biological laser is an emerging technology that started about 20 years ago (the earliest demonstration can even be dated back to 1970s^[1]) and has recently attracted tremendous research due to its potential in biomedical and biological applications.^[2–6] The definition of the biolaser is evolving over the past few years, but the generally accepted one nowadays is a biolaser or biological laser is a new type of laser that has biological materials as part of its gain medium and/or part of its cavity, or that is embedded/integrated within biological materials.^[6] As compared to fluorescence, the laser emission is advantageous due to its strong light intensity (which leads to a high signal to noise ratio), possibility of directional out-coupling (and hence ease of detection and a high signal to noise ratio), optical feedback mechanism (hence high sensitivity towards small changes in biological processes), threshold behavior (which results in strong background rejection and a high contrast ratio in imaging), and narrow linewidth (which leads to spectrally multiplexed detection/imaging/tracking). Biolasers initially utilized biological materials (such as cells) passively, and detected and imaged intracellular changes by placing cells inside a laser cavity.^[2,7,8] In the past decade, dyes, quantum dots, quantum wells, nanowires, rare-earth materials, fluorescent proteins, fluorescent product resulting from enzyme–substrate

reaction, and other naturally fluorescent biomaterials have been used to participate actively in lasing action.^[4,5,9–17] Biolasers have been employed in the detection of various bioactivities at the molecular,^[18–29] cellular,^[5,30–33] and tissue levels.^[34–36] Recently, their applications in cell tracking,^[12,15,16,37] labeling/probes,^[14,38–40] implantable devices,^[41] cell/tissue imaging^[5,31,35,40,42–46] start to emerge.

The most recent review and perspective paper on the biolaser was published 5 years ago.^[6] Since then, a tremendous

amount of research has been undertaken with a significant number of papers published. In particular, the first Gordon Research Conference entitled “Lasers in Micro, Nano, and Bio Systems” was held in 2018^[47] and the second one expected to be held in 2021, heralding the emergence and highlighting the importance of the biolaser field. In this article, we will discuss various biolasers and their potential biological and biomedical applications with the focus on the work done after 2014. We divide this article into four sections titled “Key Factors for Laser-Based Detection,” “Biological and Biomedical Sensing,” “Cell Labeling/Tracking and Implantable Devices,” and “Imaging and Mapping.” There are certainly some overlaps among those sections. Such categorization represents merely our own choices. In the end, we will discuss briefly the possible future directions of the biolaser.

2. Key Factors for Laser-Based Detection


Laser-based detection is fundamentally different from fluorescence-based one. In this section, we highlight the advantageous features of laser-based detection and discuss the issues that we should consider when we design and develop biolasers.

2.1. Sensitivity

Sensitivity is regarded as one of the most important factors in biosensing applications. Due to the lasing threshold behavior and optical feedback mechanism, small changes in underlying biological processes are significantly enhanced in the laser emission, which, together with strong (and possibly directional) laser emission, enables sensitive quantification of analytes. Furthermore, since laser emission is coherent, it can be coupled out of the cavity with high efficiency whereas incoherent fluorescence is blocked by the highly reflective mirror in the cavity. As a result, a high signal (i.e., laser emission) to background/noise (i.e., residual fluorescence background below the lasing threshold) ratio can be achieved, which usually exceeds 100.

Prof. Y.-C. Chen
School of Electrical and Electronics Engineering
Nanyang Technological University
50 Nanyang Ave, Singapore 639798, Singapore
E-mail: yucchen@ntu.edu.sg

Prof. Y.-C. Chen, Prof. X. Fan
Department of Biomedical Engineering
University of Michigan
1101 Beal Ave., Ann Arbor, MI 48109, USA
E-mail: xsfan@umich.edu

 The ORCID identification number(s) for the author(s) of this article can be found under <https://doi.org/10.1002/adom.201900377>.

DOI: 10.1002/adom.201900377

2.2. Spectral Resolution and Multiplexity

The extremely narrow laser emission linewidth is being explored for spectrally multiplexed detection/imaging/labeling and cell tracking.^[12,15,16,37,48,49] In contrast to fluorescence, which usually has a spectral linewidth of ≈ 50 nm, the laser emission linewidth is far below 1 nm (in many cases, it is limited by the spectrometer's spectral resolution). Consequently, multiple spectrally distinguishable laser lines from different fluorophores can coexist within a spectral band. For example, 4–5 spectrally distinguishable laser emission from 4 to 5 different green emission dyes can be achieved within a band of only ≈ 50 nm,^[43] although the fluorescence from those green dyes are extremely difficult to distinguish spectrally. The reason for the above phenomenon is that the spectral position of the laser emission is determined jointly by the fluorophore's emission spectrum and absorption spectrum, as well as the cavity length (in contrast, the spectral position of fluorescence is determined solely by the fluorophore's emission spectrum). Similarly, thousands of spectrally distinguishable semiconductor quantum well lasers of micrometer and sub-micrometer in size were used to track cells.^[12,15,16] Besides spectral multiplexing, laser emission provides several optical characteristics not available in fluorescence, such as the lasing threshold, the spatial distribution of a lasing mode, lasing-mode competition, and lasing-gain clamping, as well as polarization, which can be explored for multiplexed detection.

2.3. Spatial Resolution and Signal Contrast

Spatial resolution and imaging contrast are important in the field of optical imaging. In contrast to regular fluorescence-based imaging that usually provides "spatially blurred" signal to cover a large area with a low spatial resolution and a low contrast between the sites with high and low biomarker expressions, the laser-based imaging can significantly improve the image contrast and lateral and axial resolution^[13,43] due to the fundamental differences between the laser emission (which is coherent emission and strong/directional, and has lasing threshold behavior and background rejection capability) and fluorescence (which is incoherent emission).

2.4. Biocompatibility and Cavity Compatibility

When designing biolasers for cell labeling/tracking and implantable devices, biocompatibility and biodegradability should be considered, which includes the toxicity of the laser materials, biofouling, and dye concentration. The size of the laser should be as small as possible to avoid any unwanted effect on cell functions. As discussed in the next section, there are a plethora of cavity configurations available that have different spectral profiles (e.g., high transmission at one spectral band and high reflection at another), Q -factors (ranging from 100s to >1 million), and geometries (e.g., planar and circular). The choice of the cavity depends on the applications. For example, for imaging the planar structure may be preferred and for intracellular labeling and tracking, ring-shaped and spherical cavities are more commonly used due to their compact sizes. In addition, in



Yu-Cheng Chen received his B.S. in Optics from National Central University, Taiwan in 2010 and M.S. in Optoelectronics from National Taiwan University (NTU), Taiwan in 2012. From 2012 to 2015, he worked as a research scientist at the Molecular Imaging Center at NTU-Hospital, Taipei. He received a Ph.D. degree in

Biomedical Engineering from the University of Michigan, Ann Arbor, USA in 2017 and worked as a postdoctoral fellow until July 2018. Since 2012, he has coauthored more than 40 scientific journals/proceedings articles, where much of his research was widely reported. His research mainly focuses in optofluidics, biolasers, nanophotonics, ultrafast biophotonics, biosensors, and medical imaging. Currently, he is a Nanyang Assistant Professor at Nanyang Technological University in Singapore.



Xudong Fan obtained B.S. and M.S. degrees from Peking University, China, in 1991 and 1994, respectively, and Ph.D. from the University of Oregon, USA, in 2000. He is Professor of College of Engineering and School of Medicine at the University of Michigan, the Director of NIH Microfluidics in Biomedical Sciences Training Program, Thrust

Leader of the Center for Wireless Integrated MicroSensing and Systems, and Associate Director of Michigan Center for Integrative Research in Critical Care. His research lies in the interface of photonics, engineering, microfabrication, microfluidics, and biomolecular analysis, instrumentation, and biomedicine. In particular, his lab is pursuing ultrasensitive optical label-free sensors, microfluidic lasers, optofluidic biolasers, high-performance microgas chromatography devices, breath analysis for disease diagnosis/prognosis, rapid microfluidics bioassays, miniaturized vapor sensors, wearable devices, and ultrasound detection. He has over 160 peer-reviewed publications and ~ 30 issued/pending patents. He is Fellow of Optical Society of America, SPIE, and Royal Society of Chemistry.

many applications, the compatibility with microfluidics should be considered for dynamic control of experimental conditions.

3. Biological and Biomedical Sensing

Laser emission-based detection relies on the laser cavities, which provide optical feedback and hold or are surrounded by

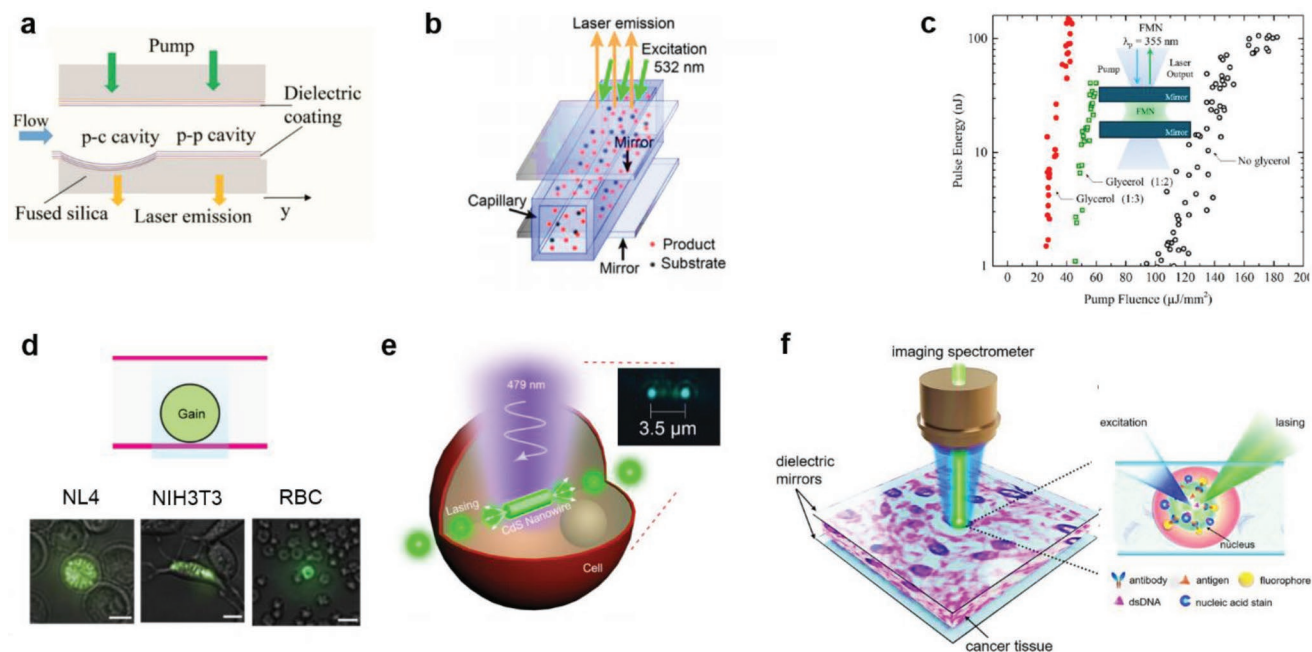


Figure 1. a) An FP cavity with the plano-concave design (left) and the plano–plano design (right). Adapted with permission.^[50] Copyright 2015, Royal Society of Chemistry. b) Structure of the FP cavity with a microfluidic channel in between. Adapted with permission.^[53] Copyright 2017, Elsevier. c) Threshold curves for the FMN laser with and without glycerol. The inset shows the FP cavity. Adapted with permission.^[56] Copyright 2016, Optical Society of America. d) Single cell lasers with an FP cavity using different cell lines, including NL4, NIH3T3, and red blood cell. Adapted with permission.^[30,51] Copyright 2015, Wiley-VCH and Optical Society of America. e) Intracellular lasers with a nanowire inside a cell. The two facets of the nanowire serve as the two reflectors and form an FP cavity. Adapted with permission.^[14] Copyright 2017, Royal Society of Chemistry. f) Schematic of tissue lasers utilizing an FP cavity formed by two highly reflective dielectric mirrors, in which cells or tissues labeled with specific probes are sandwiched in between. Adapted with permission.^[43] Copyright 2017, Springer Nature.

biological samples/materials. Depending on the applications, optical cavities can vary from planar Fabry–Pérot (FP) cavities to circular-shaped microsphere and ring resonators. In this section, we will describe six types of commonly used laser cavities and their applications in biological and biomedical sensing.

3.1. Fabry–Pérot Cavity Laser Based Biosensing

Figure 1 illustrates various FP microcavities, in which the biological gain medium can be sandwiched between two highly reflected mirrors. The FP cavity provides a whole-body interaction between the light and the gain medium, i.e., a predominant portion of the optical field is within the body of the gain medium, in contrast to the evanescent interaction in ring resonator sensors or plasmonic sensors. This arrangement is particularly attractive when the gain medium is inside a specific localization of a cell or tissue. One of the challenges in the FP cavity is the alignment of the two mirrors. A few schemes have been demonstrated to maintain a high *Q*-factor. As shown in **Figure 1a**, a planoconcave FP cavity was developed to improve cavity stability and a high *Q*-factor close to 10^6 was achieved.^[50] Spherical cells and microspheres can also be used to provide the lensing effect and the lateral confinement to mitigate the *Q*-factor degradation caused by mirror misalignment.^[5,30,51,52]

With the advantage of the planar configuration, the FP cavity is suitable for various applications, especially on-chip devices and imaging. In 2014, Wu et al. demonstrated an enzyme linked

immunosorbent assay (ELISA) laser for biodetection with significantly improved dynamic range,^[9] in which the fluorescent product resulting from the enzyme-substrate reaction was used as the gain medium. Similar work was later carried out by Gong et al. and Yang et al., showing the applications of the biolaser in sensitive sulfide ion detection^[53] (**Figure 1b**) and turbidimetric inhibition immunoassay,^[54] both of which had a larger dynamic range than the traditional methods. Besides immunoassay, Hou et al. developed DNA high-resolution melting (HRM) analysis by using the FP cavity based biolaser.^[55] Compared to the fluorescence-based HRM, the laser-based HRM has advantages of higher emission intensity for a better signal-to-noise ratio and a sharper transition for better temperature resolution. In **Figure 1c**, Rivera et al. developed an FP based biolaser using flavin mononucleotides (FMNs) as the gain medium,^[56] which was subsequently used for biochemical detection such as oxygen sensing.

The FP cavity can also be used for cell lasers,^[5,30,31,51] in which the cell (or cells) are placed between the two mirrors and are stained with or immersed in fluorophores that serve as the gain medium, as shown in **Figure 1d**. Lasing spectra and mode profiles are used to analyze the cells. The FP cavity is further used in a nanowire laser,^[13,14] as exemplified in **Figure 1e**, whose facets act as two mirrors due to the large refractive index contrast between the nanowire and the environment. The nanowire laser is usually used as an intracellular probe to detect the changes in cytoplasm (see more details about the intracellular probes in Section 4).

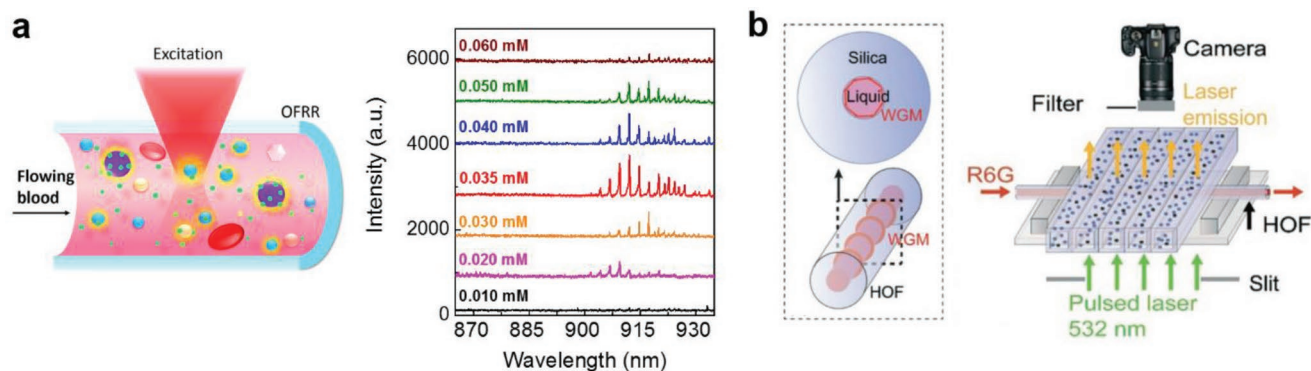


Figure 2. Optofluidic ring resonator (OFRR). a) OFRR laser in human whole blood by using FDA approved dye, indocyanine green (ICG), to detect lipoproteins and albumins. Adapted with permission.^[34] Copyright 2016, The Optical Society. b) Reproducible OFRR laser for chip-scale arrayed biochemical sensing. The left inset shows a hollow fiber that serves as the WGM laser cavity. Adapted with permission.^[65] Copyright 2018, Royal Society of Chemistry.

Finally, advancing to the tissue level, several tissue lasers have been demonstrated in recent two years, in which a thin flat tissue was sandwiched between the two mirrors (Figure 1f).^[42–44,48] The tissue can be labeled with dyes that target specific sites inside the tissue (e.g., boron-dipyrromethene (BODIPY) for adipose cells, YOPRO for nuclear acids, and antibody-conjugated dyes for proteomic biomarkers). By scanning the pump laser over the tissue, the image of the laser emission can be mapped (see details about laser emission-based imaging in Section 5).

3.2. Whispering Gallery Mode Laser Based Biosensing

The whispering gallery mode (WGM) laser cavities can be constructed in the form of solid cylinders,^[57] circular-shaped capillaries,^[22] microspheres,^[58] microdroplets,^[59,60] microdisks,^[16,61] ring-shaped waveguides,^[62,63] and rectangular shaped rods.^[49] The WGM cavity relies on the total internal reflection at the curved boundary to provide optical feedback. It usually has a high Q -factor ($>10^7$), which leads to a low lasing threshold, and is compact as compared to other types of cavities.

One of the WGM cavities is called optofluidic ring resonator (OFRR), which is a thin-walled glass capillary that serves as both ring resonator and the microfluidic channel. Several promising applications have been demonstrated in the past few years, including differentiation between proteins FRET pairs^[20] and lasing in human blood with indocyanine green (Figure 2a).^[34] However, while the OFRR can be fabricated in lab easily at a low cost, it is less reproducible in terms of size and the wall thickness using a lab-based CO₂ laser pulling machine, which hinders mass production of the OFRR. Recently, highly reproducible OFRRs have been achieved using an industrial fiber draw tower.^[64–66] A laser array based on those OFRRs also demonstrated the potential for high throughput biosensing (see Figure 2b).

Microdroplets, microbeads, and microdisks are also commonly used for the biolaser cavity. Figure 3a shows a microsphere laser using intramolecular charge-transfer (ICT) dye as the gain medium.^[67] The lasing wavelength can be switched back and forth when protonic acids bind to the ICT molecules, which enhances the ICT strength of the dye and

leads to a red-shifted gain. Wei et al. discovered that the natural spherical structure in starch can also act as a WGM cavity for biological sensing by encapsulating guest organic laser dye into the interhelical structure of starch granules (Figure 3b).^[68] The lasing signal could be affected by the hydration and structural transformation of the starch matrix, providing a new tool for monitoring of subtle plant biological process. In addition to organic materials, liquid crystal (LC) droplets have been investigated for biosensing or thermo-sensing to the surrounding environment.^[41,69–72] In fact, WGMs can be achieved in droplets made out of almost any LC, including smectic, ferroelectric, cholesteric, and discotic.^[71] The binding of molecules to the surface of liquid crystal droplets will in turn change the electrical properties and alignment of the inner structure, resulting in different laser emission wavelength and laser modes.^[70,73] Figure 3c is an example of an LC droplet laser used for pH and 4'-pentyl-biphenyl-4-carboxylic acid (PBA) sensing. The changes of laser spectrum and laser modes were used for characteristics of biosensing. For more examples of microsphere, microdisk, and microdroplet based lasers, see Section 4.

3.3. Photonic Crystal Laser Based Biosensing

Photonic crystals have 1D or 2D periodic nanostructures that provide tight light confinement and extremely high Q -factors as high as 10^6 . By adding a gain medium to the nanostructure, the nanocavity infiltrated with dye solution provides the optical feedback for lasing (see Figure 4a).^[24,74] The photonic crystal lasers are sensitive to the change with environmental index and surface charge. In other words, the index change can be sensed from the precise wavelength shift of photonic crystal laser emission. Such a shift observed when the photonic crystal laser was operated in liquids with different refractive indices can be used for biosensing. The bulk sensitivities for these liquids are 300–400 nm per refractive index unit (RIU) with the nanoslot. In addition, extreme high sensitivity and high specificity was achieved by using bovine serum albumin (BSA) and biotin-serum albumins.^[75] It was also demonstrated that functionalizing the photonic crystal laser surface with an antibody, the specific binding of target antigen is detected with a detection limit 2–4 orders better than that achieved by current standard methods.^[76] Recently,

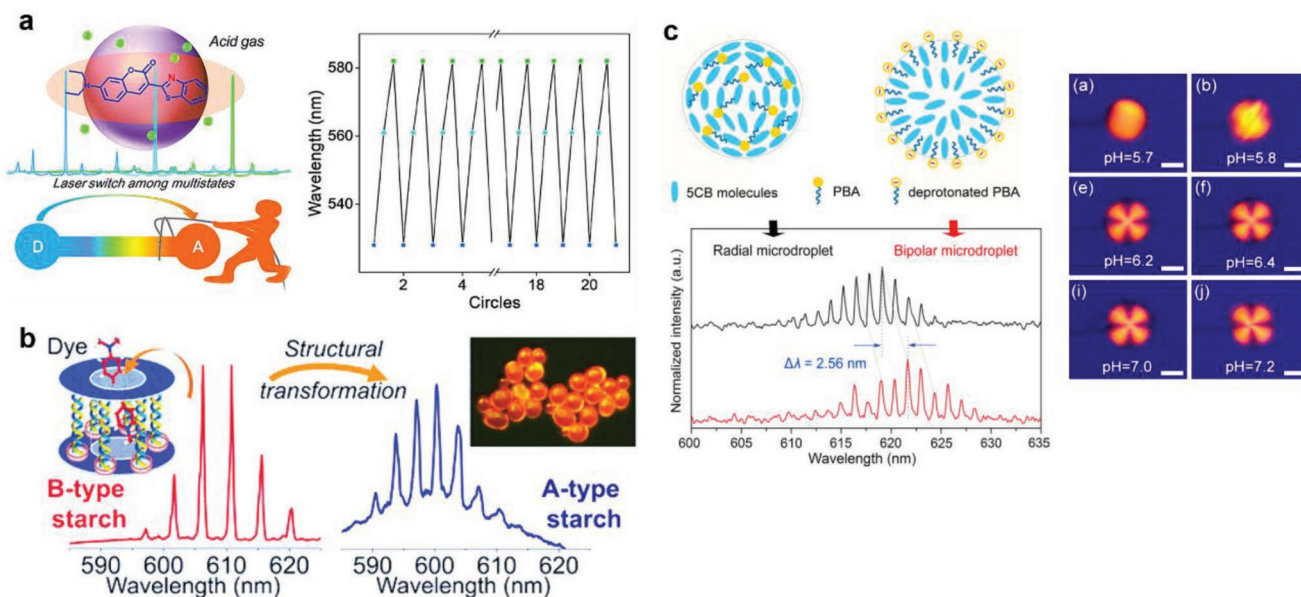


Figure 3. a) Design and illustration of a stimuli-responsive ICT molecule and microspheres. The right panel shows that lasing wavelength switches back-and-forth upon binding of protonic molecules. Adapted with permission.^[67] Copyright 2018, American Chemical Society. b) Starch as the host to build dye@starch microspheres by encapsulating guest organic laser dye into the interhelical structure of starch granules. The laser signal responds to the structural transformation of the starch matrix. Adapted with permission.^[68] Copyright 2017, American Chemical Society. c) Schematic of structural transition of PBA-doped 5CB microdroplets. The corresponding WGM lasing spectra with radial (black line) and bipolar (red line) configurations. The right panel shows that the laser mode changes for different pH values. Adapted with permission.^[70] Copyright 2018, Elsevier.

label-free and spectral-analysis-free detection of neuropsychiatric disease biomarkers using an ion-sensitive photonic-crystal laser biosensor was also achieved.^[77] Photonic crystal lasers can also detect negatively charged DNA, IgG, and PSA from their emission intensity changes or wavelength shift (see Figure 4b).^[78] Photonic crystal cavities have beneficial characteristics such as high *Q*-factor and small mode volume, which are particularly attractive for low-copy-number biosensing.

3.4. Distributed Feedback Laser Based Biosensing

Distributed feedback laser (DFB laser) relies on the 1D periodical structures to provide optical feedback with the gain material. When biomolecules of interest interact with the surface of a DFB laser, the laser wavelength shifts, which

can be used for biosensing.^[79–82] For instance, Lu et al. demonstrated the capability of a DFB laser to detect 3.4×10^{-9} M (60 ng mL^{-1}) of human immunoglobulin G (IgG) proteins and microparticles.^[83] Retolaza et al. developed an organic DFB laser to specifically detect ErbB2 protein biomarker down to 14 ng mL^{-1} (Figure 4c).^[84] Strictly speaking, the above two DFB laser examples do not fall into the biolaser definition, as they act merely like passive label-free optical biosensors. Very recently, McConnell et al. developed a sequence-selective detection of analytes (oligodeoxyribonucleotide, ODN) using a hybrid DNA/organic laser in conjunction with Ag nanoparticles.^[25] As binding occurs, the nanoparticles increase the optical losses of the laser mode through plasmonic scattering and absorption, which in turn results in an increased lasing threshold. By monitoring the lasing threshold, ODN as low as 11.5×10^{-12} M of could be detected.

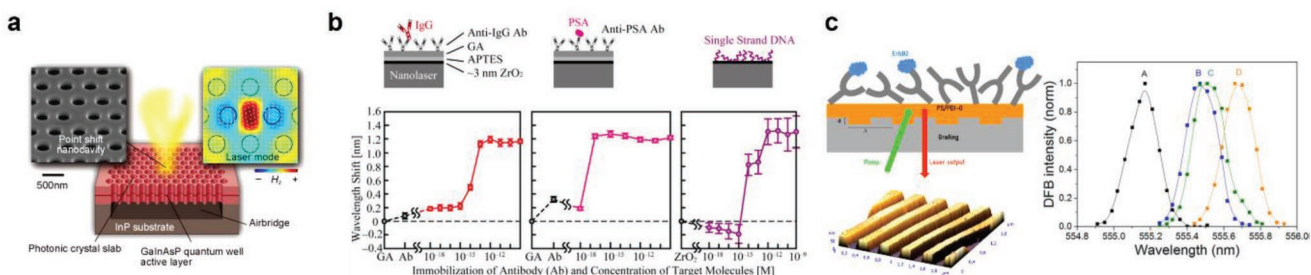


Figure 4. a) Conceptual illustration of a photonic crystal laser. Adapted with permission.^[24] Copyright 2015, Cambridge Core. b) Photonic crystal laser designed for the detection of IgG, PSA, and single-stranded DNA. Adapted with permission.^[78] Copyright 2017, Optical Society of America. c) Scheme of a DFB laser sensor. The direct capture immunoassay employed for ErbB2 biomarker detection is also shown. The right panel shows the laser peaks before functionalization, after functionalization with anti-ErbB2, after BSA blocking, and after analyte addition at a concentration of 10 ng mL^{-1} . Adapted with permission.^[84] Copyright 2016, Elsevier.

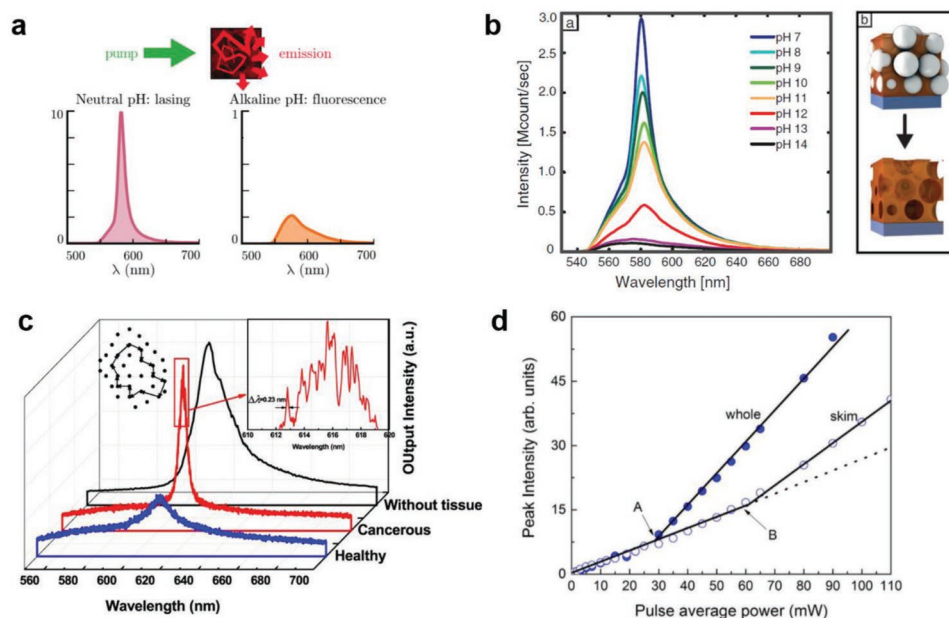


Figure 5. a) Illustration of random-laser based sensing. Multiple light scattering in the gain medium leads to amplification and lasing. Narrow linewidth (lasing) is observed when the pH value is neutral, while broad fluorescence emission is observed when it has alkaline pH values. Adapted with permission.^[87] Copyright 2017, American Physical Society. b) Biocompatible random lasing spectra from a rhodamine-doped silk random laser in aqueous solution with various molarities of NaOH dissolved in the solution that changes the solution pH. The right inset shows a sketch of the direct and inverse structure of silk. Adapted with permission.^[89] Copyright 2016, Wiley-VCH. c) Comparison of random lasing spectra of cancerous tissue and healthy tissue doped with dye. Adapted with permission.^[93] Copyright 2017, Springer Nature. d) Response of a random laser to skim and whole fat milk mixed with dye. Adapted with permission.^[94] Copyright 2016, Springer Nature.

3.5. Random Laser Based Biosensing

A random laser does not have a fixed optical cavity, but rather utilizes multireflections from highly scattered medium (such as particles) dispersed in the lasing active material to provide optical feedback for laser generation.^[36,85,86] The Q -factor of the random laser is comparatively low and the unpredictable lasing peak and lasing threshold remain a problem. Nevertheless, the ability to generate lasing in biological materials without any external cavities is definitely a huge advantage. The spectral characteristics of the laser emission are strongly dependent on the scattering properties of the medium, providing new tools to investigate disordered biological materials. To date, random lasers have shown the feasibility to detect physical changes or chemical changes within biological materials.^[87,88] **Figure 5a** shows the sensing mechanism of a random laser, by using pH sensing as an example. In **Figure 5b**, a biocompatible silk random laser was achieved by nanostructured silk protein matrices.^[89] Lasing action was revealed by spectral narrowing and showed a pH sensitivity exceeding by two orders of magnitude compared to a conventional fluorescence sensor. Besides pH sensing, Ismail et al. have designed random lasers to detect dopamine, an important neurotransmitter for neurological disease.^[90] The gold nanoparticles were used to scatter the light while dye served as the laser gain medium. Dopamine with copper ions triggers the aggregation of gold nanoparticles and thus affects laser properties such as lasing intensity, linewidth, and threshold to achieve highly sensitive neurotransmitter detection. For biomedical diagnosis, Polson et al. demonstrated a random laser by infiltrating the tissues

with dyes (**Figure 5c**).^[35] Due to the different scattering properties, the cancerous and healthy tissue can be distinguished by their lasing spectra.^[91–93] Other lasing characteristics were also explored for laser based detection. For example, Abegão et al. used the difference in the lasing threshold to detect fat content in milk (**Figure 5d**)^[94] using random lasers.

3.6. Plasmonic Laser Based Biosensing

Plasmonic lasers (also known as spasers) are a class of coherent light sources that use metallic nanoparticles for light localization and amplification based on surface plasmon resonance. Plasmonic lasers exploit this confinement effect to deliver intense optical energy below the diffraction barrier on extremely fast time scales.^[38,95,96] The interface between dyes (molecules) and metals creates strong laser emission that can be applied in biomolecular sensing. **Figure 6a** shows the first demonstration of a plasmonic laser particle. A major advantage of the plasmonic laser is its nanometer size, which is smaller than the lasing wavelength. Therefore, the plasmonic laser can be an excellent candidate for intracellular labeling and sensing. However, plasmonic lasers suffer from extremely low Q -factors and thus often require high pump intensities and/or high concentrations of dye to reach lasing conditions.

Another format of the plasmonic laser is based on metallic structures on a chip. In **Figure 6b** Ma et al. demonstrated the sensing capability of a plasmonic laser consisting of a single crystalline semiconductor CdS nanoslab on top of an Ag surface, separated by a MgF₂ layer.^[97] The Odom group reported on how

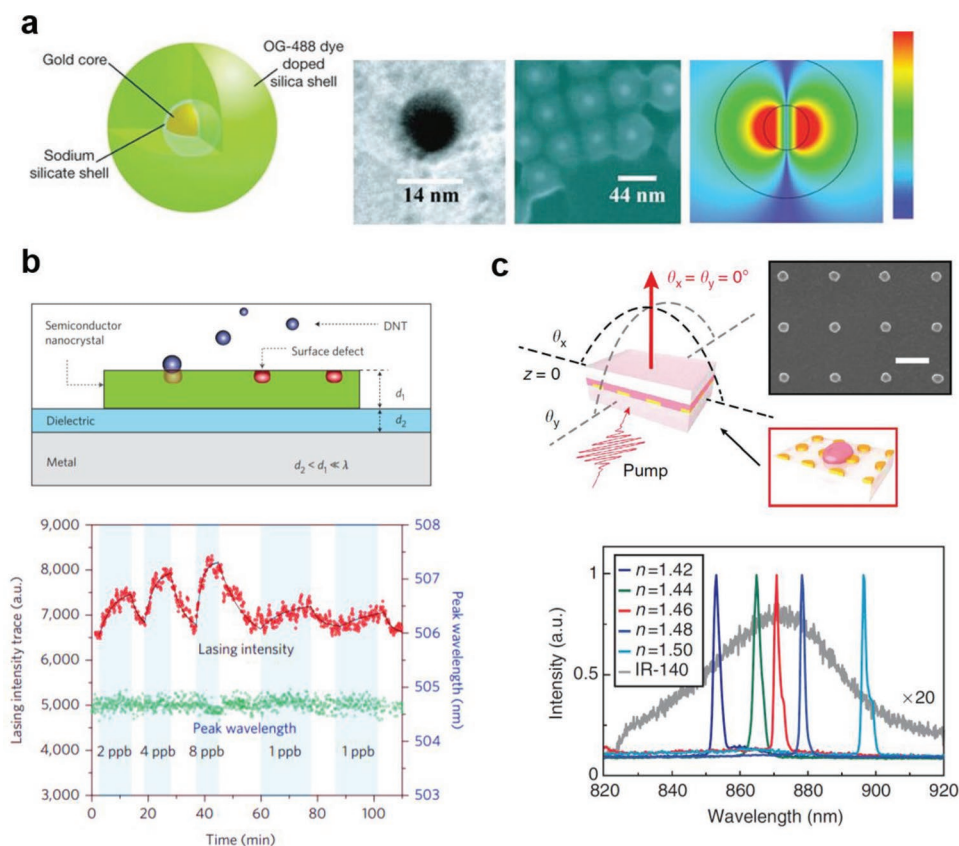


Figure 6. a) Structure of a plasmonic laser. A gold core surrounded by a silica shell filled with green dye. The corresponding scanning electron microscope images show that the gold core and the thickness of the silica shell were about 14 and 15 nm, respectively. A simulation of the plasmonic laser on the right shows the device emitting visible light at 525 nm. Adapted with permission.^[96] Copyright 2009, Springer Nature. b) Schematic of a plasmonic laser-based sensor. The bottom figure shows the continuous trace (red diamond) of the plasmonic laser emission in the presence of 1, 2, 4, and 8 ppb of DNT vapor. Adapted with permission.^[97] Copyright 2014, Springer Nature. c) Schematic and SEM image of a plasmonic laser based on gold nanoparticle array fabricated on-chip. The bottom shows the lasing peak position shifts when the surrounding liquid refractive index increases from 1.42 to 1.50. Adapted with permission.^[98] Copyright 2015, Springer Nature.

the lasing based on band-edge lattice plasmons can be spectrally tuned in real time by changing the refractive index environment around the plasmonic array fabricated on a chip (Figure 6c).^[98] This phenomenon in turn can be used for refractive index sensing by tracking the lasing wavelength. In contrast to its nanoparticle counterpart, the on-chip plasmonic lasers are still quite large. Therefore, it is difficult to use them in intracellular applications.

In general, the plasmonic lasers as a new laser platform have unique properties unavailable to dielectric lasers discussed previously. However, to date their applications in biochemical sensing, imaging, and labeling are still relatively scarce. More investigations are needed to realize the full potential of the plasmonic laser.

4. Cell Labeling/Tracking and Implantable Devices

There are increased research activities dedicated to the development of various lasing particles for labeling and tracking of biomolecular and cellular activities and for imaging contrast agents with the particle size ranging from the micrometer scale to the nanometer scale.

Figure 7 shows a few exemplary schemes that use micro-/nanolasers for labeling. The first intracellular laser at the micrometer scale was achieved by Humar et al. and Schubert et al. in 2015, where dye-doped polystyrene microbeads and oil microdroplets were used as a hard and soft WGM cavity, respectively (Figure 7a).^[46,99] The experiments were performed in both in vitro cells and ex vivo porcine adipose tissue. Later on Schubert et al. further demonstrated the feasibility of intracellular laser-based cell tracking by establishing routes for robust and efficient introduction of the lasing particles into a wide range of cells, including primary cells and cells from the nervous system (Figure 7b).^[45] For deep tissue imaging and labeling, more recently Lv et al. developed microbead lasers of 2–10 μm in diameter that have near-infrared emission (around 700 nm) and low lasing thresholds (Figure 7c).^[37] Those microlasers were then uptaken by macrophages, delivering excellent WGM lasing for cellular labeling during transformation of normal macrophages to foamy ones. Recently, Fernandez-Bravo et al. developed a continuous-wave upconverting laser particle by coating Tm^{3+} -doped energy-looping nanoparticles (ELNPs) onto a polystyrene microbead.^[39] The microlasers formed by 5 μm polystyrene beads mixed with exotic materials could reliably

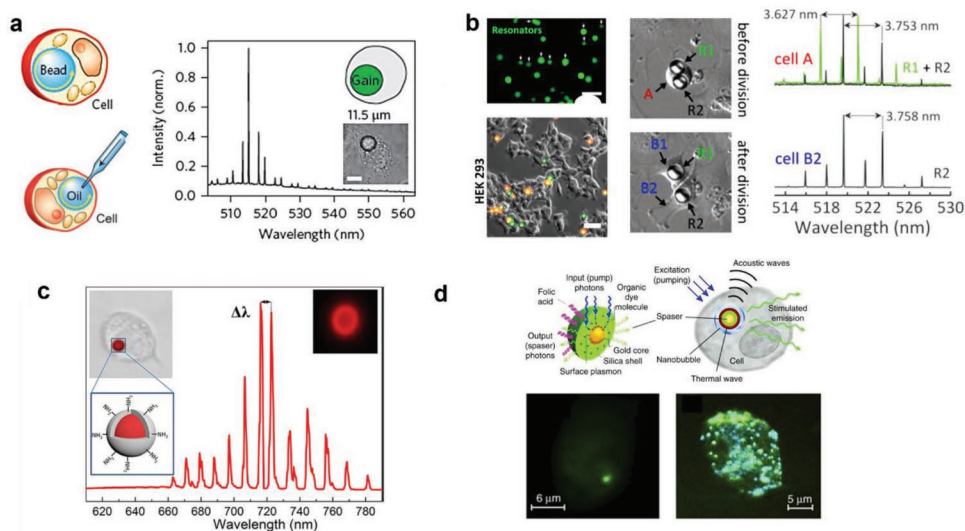


Figure 7. a) Schematic of a bead internalized by a cell and of the injection of oil into a cell to form a microdroplet laser. The laser emission spectra from a fluorescent polystyrene bead inside a cell is provided on the right. Adapted with permission.^[99] Copyright 2015, Springer Nature. b) Long-term tracking of 3T3 fibroblasts over several cell generations. The right panel shows lasing spectra of microbeads inside the mother cell and after cell division (top/bottom). Adapted with permission.^[45] Copyright 2017, Springer Nature. c) Intracellular near-infrared microlaser probes based on organic microsphere–SiO₂ core–shell structures for cell tagging and tracking. Adapted with permission.^[37] Copyright 2018, American Chemical Society. d) Schematic of a plasmonic lasing nanoparticle as multimodal cellular nanoprobe shown in the top panel. Comparison of the fluorescence image of breast cancer cells (MDA-MB-231) with a single plasmonic lasing nanoparticle and multiple plasmonic lasing nanoparticles is shown in the bottom panel. Adapted with permission.^[38] Copyright 2017, Springer Nature.

emit bright light on specific wavelengths when exposed to infrared light. The concoction makes light bounce around the inner surface of the bead, creating collisions that can repeatedly amplify the light.

One of major issues with the micrometer-sized lasers is their relatively large size, which may potentially affect cell biofunctions. Therefore, laser particles of smaller sizes towards the sub-micrometer scale or even the nanometer scale become attractive for cellular labeling.^[12,14,16,38,100] Figure 1e shows the nanowire laser probe that has about 250 nm in diameter and a few micrometers in length. By monitoring the lasing peak wavelength shift in response to the intracellular refractive index change, the nanowire laser probe shows a sensitivity of 55 nm per refractive index unit (RIU) and a figure of merit of ≈ 98 .^[14] Very recently, whispering gallery mode (WGM) lasers based on 10–20 μm diameter polystyrene beads were introduced into beating cardiomyocytes to realize all-optical recording of transient cardiac contraction profiles with cellular resolution.^[100] Figure 7d shows the smallest nanolaser particle based label (≈ 22 nm in diameter) to date that is formed by a plasmonic gold nanoparticle with a silica shell doped with highly concentrated DCM dye. This nanolaser was used in flowing blood of animal models and tissues *in vivo*.^[38]

The rich lasing spectra and extremely narrow lasing linewidth provide uniquely identifiable spectral fingerprints that enable massive labeling and subsequent tracking of cells.^[12,16,37,45,46,99] For example, Martino et al. and Fikouras et al.^[12,16] have developed semiconductor microdisk lasers shown in **Figure 8a**. To ensure chemical and optical stability and reduce potential toxicity from the semiconductor materials, a biologically inert coating, silica shell, was used. Slightly different diameters of the microdisks result in different lasing wavelengths, which

can be used to label and track different cells. Sharp laser emissions with single-mode lasing over a broad range in the near-infrared (**Figure 8b**) region as well as the visible region were achieved. Those microdisk lasers with various lasing wavelengths were safely uptaken by several cell types *in vitro* and monitored over 24 h (**Figure 8c**). Thanks to their small sizes, each cell can internalize multiple microdisks for multiplexed laser emission spectrum, thus allowing to uniquely label an even larger number of cells. Those lasing microdisks are particularly attractive for applications requiring nonobstructive tagging of cells for studying cell migration in cancer invasion and immune response (**Figure 8d**).^[12] Finally, real time tracking of thousands of individual cells in a 3D tumor spheroid demonstrated the stability and biocompatibility of these probes *in vitro* and their utility for wavelength-multiplexed cell tagging and tracking (**Figure 8e**). High motility and low motility of tumor cells were clearly tracked via microdisk lasers.

In addition to labeling and tracking, micro/nanolasers have been exploited for potential use as implantable devices and optogenetic stimulation.^[39,41,58] For example, implantable microlasers made of biocompatible materials such as BSA, pectin, cellulose, poly-lactic acid (PLA) crystals, and upconversion nanoparticles are shown in **Figure 9a–c**. Furthermore, recent work has shown that the micro/nanolasers can be used for photoacoustic imaging.^[38,40] For example, Li et al. demonstrated the ultrasound modulated droplet lasers (**Figure 9d**), in which the laser intensity from an oil droplet can be reversibly enhanced when the ultrasound pressure is beyond a certain threshold.^[40] Additionally, it was shown that the ultrasound modulated droplet lasers could work well in vessels containing human whole blood, which promises the future applications in sensing and imaging.

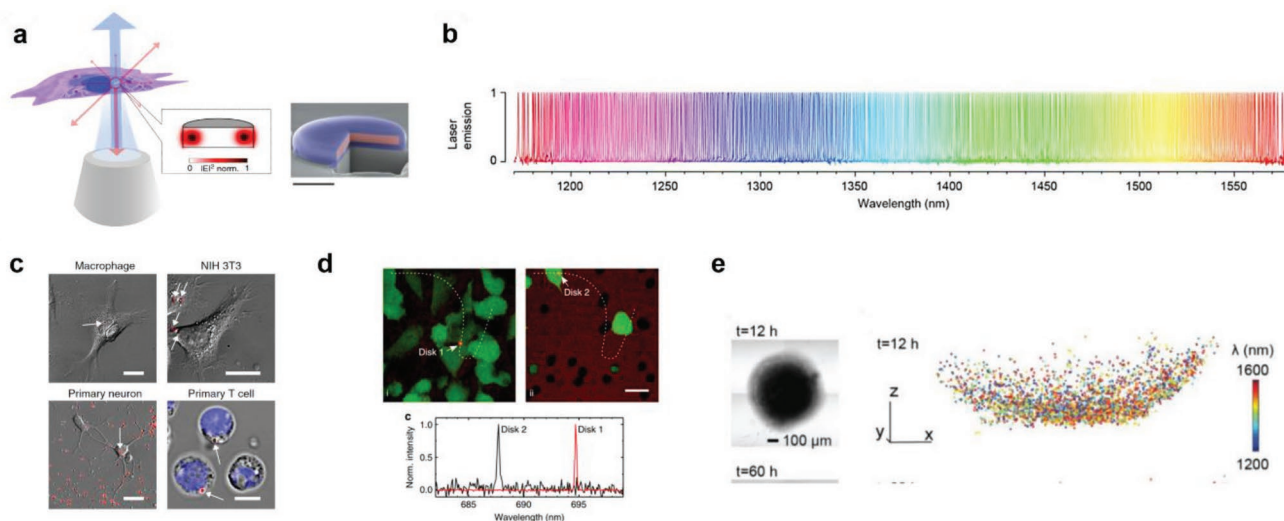


Figure 8. a) Conceptual illustration of a semiconductor microdisk laser internalized into a cell. The right panel shows the microdisk protected by a biocompatible silica shell. Adapted with permission.^[12,16] Copyright 2018 and 2019, Springer Nature. b) Highly multiplexed microdisk lasers. Normalized laser emission spectra of 400 microdisk lasers from 1170 to 1580 nm with an interval of ≈ 1 nm. Adapted with permission.^[16] Copyright 2019, Springer Nature. c) Cellular uptake and lasing from semiconductor microdisks having a sub-micrometer diameter. Differential interference contrast microscopy of primary human macrophages, NIH 3T3 cells, primary mouse neurons, and primary human T cells with internalized microdisks (overlaid red fluorescence, indicated by white arrows). Nucleus of T cells labeled with blue Hoechst dye. Adapted with permission.^[12] Copyright 2018, Springer Nature. d) Top: Migration of cells with microdisk lasers through a microporous membrane captured under scanning confocal microscopy. Bottom: The corresponding lasing spectra of disks 1 and 2 recorded in parallel with confocal microscopy. Adapted with permission.^[12] Copyright 2018, Springer Nature. e) Cell tracking in a tumor spheroid. Left: Optical transmission image of the tumor spheroid at 12 h. Right: Spatial distribution of micro disks inside the tumor. Each dot represents a micro disk with color coding for its wavelength. Adapted with permission.^[16] Copyright 2019, Springer Nature.

5. Imaging and Mapping

Lasing emission can further be used for imaging, which provides 2D spatial information of the biological material in addition to spectral information. Such spatial information reveals the gain distribution and morphological changes of cells or tissues. Early work to map lasing emission was conducted in 2004, where Polson et al. used a random laser generated from tissues to map and distinguish cancerous and healthy tissue from patients.^[35,91] However, the spatial resolution was more than 1 mm, which could not accurately reveal subcellular features. In addition, the random laser is less controllable in the lasing threshold and does not provide biomolecular information. Recently, two laser emission-based imaging techniques were proposed and demonstrated. The Yun group proposed and demonstrated using a perovskite nanowire as a biological probe for laser imaging (Figure 10a),^[13] which has a narrow lasing spectral linewidth, subdiffraction resolution, and low out-of-focus background. The Fan group developed the scanning laser-emission-based microscope (LEM) that maps lasing emission from nuclear biomarkers in human tissues.^[43] Figure 10b illustrates the concept of the LEM, in which a tissue labeled with site-specific fluorophores (such as nucleic acid probes) and/or antibody-conjugated fluorophores is sandwiched inside an FP microcavity formed by two mirrors. One can clearly see from the right inset of Figure 10b that LEM provides a much higher spatial resolution than conventional fluorescence microscopy in a cell nucleus. Only highly localized EGFR expressions can generate lasing emission within the cell nucleus. By integrating with a scanning stage, mapping/imaging of the lasing

emission from nuclear biomarkers were achieved in human tissues with a subcellular and sub-micrometer resolution. Examples of a set of LEM images of cancerous and normal lung tissues from patients are provided in Figure 10c. Based on the different lasing thresholds between cancer and normal cells, the LEM enabled the identification and multiplexed detection of nuclear proteomic biomarkers, with high sensitivity for early-stage cancer diagnosis. To date, LEM has been used to examine other types of cancer tissues, including stomach, colon, and breast, both frozen and formalin-fixed paraffin-embedded (FFPE) tissues.^[44] Similarly, the immuno-laser that targets cancer biomarkers such as EGFR, p53, and Bcl-2 has also been achieved on tissues by conjugating the corresponding antibodies to fluorophores.^[43]

Since the LEM is able to detect the abnormal changes at the molecular level, much earlier than the morphological changes at the tissue level, it may be used for early diagnosis of cancer and cancer precursors.^[48] Recently, the Fan group used dietary controlled mouse model and imaged the lasing emission from chromatins of the colon tissues of those mice. It was discovered that, despite the absence of observable lesions, polyps, or tumors under stereoscope, high-fat treated mice exhibited significantly lower lasing thresholds than low-fat treated mice (i.e., their colon tissues are easier to lase under the same pump conditions), as shown in Figure 10d. The new findings may make the LEM a powerful tool that complements traditional hematoxylin and eosin staining (H&E) and immunohistochemistry (IHC) in early diagnosis of cancers and cancer precursors.

Besides imaging cancer cells, Chen et al. employed the LEM to record the action potentials in neurons caused by subtle transients

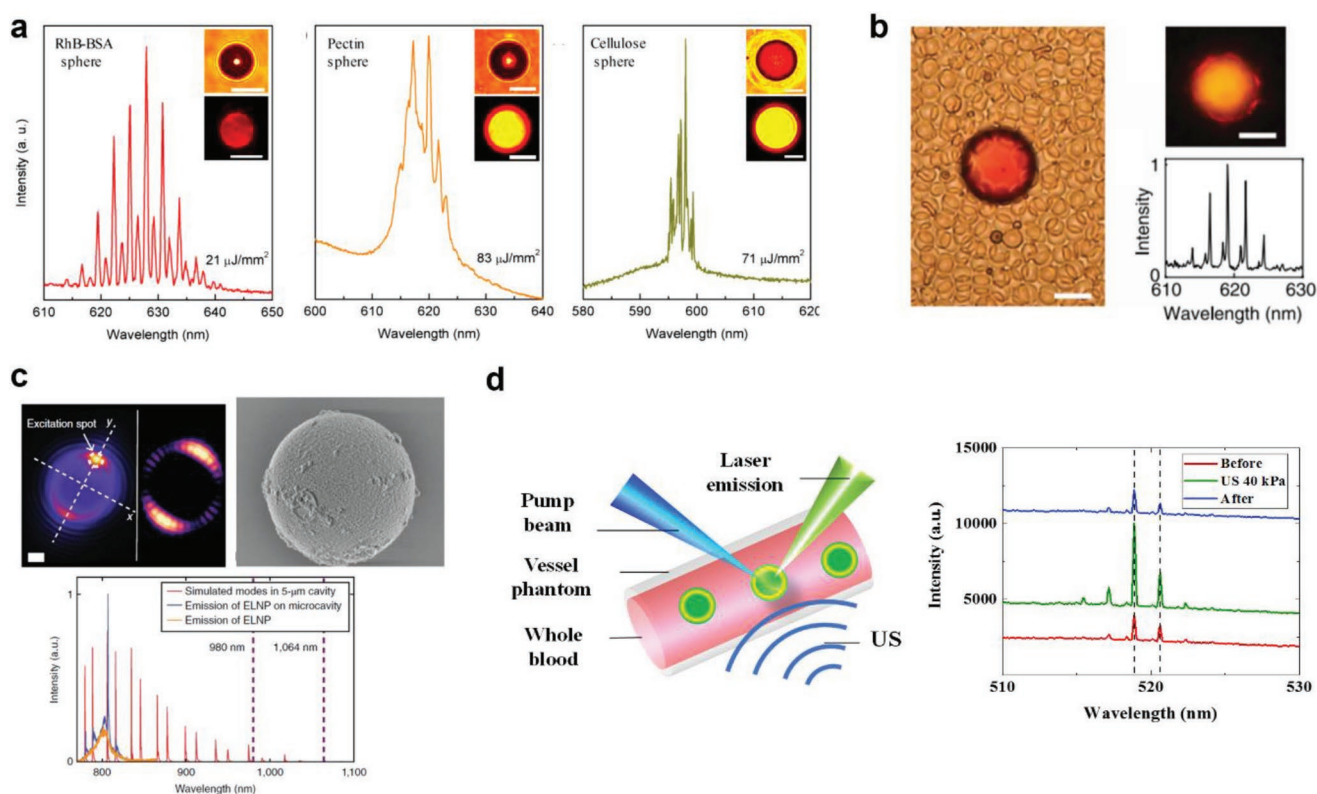


Figure 9. a) Lasing spectra from typical RhB doped BSA, pectin, and cellulose spheres, respectively. The insets show optical and fluorescence image of the corresponding spheres. Adapted with permission.^[58] Copyright 2017, Wiley-VCH. b) Microsphere laser formed by PLA and immersed in blood. The right panel shows a superimposed fluorescence and laser emission image. The lasing spectrum is also provided below. Adapted with permission.^[41] Copyright 2017, Optical Society of America. c) Left: Wide-field image of a microsphere laser displaying optical modes circulating around the cavity. Excitation occurs at a diffraction-limited spot on the side of the bead, as marked by the arrow. Right: SEM image of a 5 μm diameter polystyrene bead coated with ELNPs. The bottom shows the corresponding simulated near-infrared WGM spectra overlaid on the experimental emission spectra of ELNPs and ELNP-coated beads pumped above the lasing threshold. Adapted with permission.^[39] Copyright 2018, Springer Nature. d) Ultrasound modulated microdroplet lasers in blood stream. The right panel shows the lasing emission is reversibly enhanced in the presence of ultrasound. Adapted with permission.^[40] Copyright 2018, American Chemical Society.

(Ca^{2+} concentration) in primary neurons in vitro with a subcellular and single-spike resolution^[101] (see **Figure 11a**). By recording the laser emission from neurons, it is discovered that lasing emissions could be biologically modulated by intracellular activities and extracellular stimulation with >100-fold improvement in detection sensitivity over traditional fluorescence-based measurement. An example of laser recording (imaging) of intracellular spontaneous calcium signals in neurons is provided, in which the neuron laser mode changes with time during each spiking. In addition to single cells,^[5,101] lasing from a cell array was performed.^[31] Time series cell laser measurements in the lasing peak spectral position and the lasing mode may help reveal abnormal cells that deviate from a large population of normal cells (**Figure 11b**).

6. Outlook and Challenges

As an emerging technology, there are many directions in the field of biolaser that can be explored.

1) Imaging at the cellular and tissue level will be interesting and important for biological research and biomedicine.

For example, a novel hyperspectral imaging technology can be developed that combines multiplexed (i.e., multi-wavelengths) spectral information and spatial information of laser emission as well as the laser mode profile. In addition, regular fluorescence imaging and brightfield imaging technologies can be integrated with the laser emission based imaging to provide a better and deeper understanding of the functions and behavior of cells and tissues from other perspectives. Biolasers based on a cell array in which individual cells reside in wells or flow through a microfluidic channel can be constructed for high-throughput cell analysis (especially time series analysis). Similarly, tissue arrays can also be developed for high-throughput tissue analysis. One important application of the laser emission imaging is to develop a technology that complements the existing H&E and IHC techniques for early detection of cancers and cancer precursors.

2) Due to the rich spectral characteristics available to laser emission (such as narrow lasing linewidth, lasing mode profile, and polarization, etc.), cell tagging and tracking based on lasing micro-/nanoparticles become increasingly attractive. While currently micrometer and sub-micrometer sized

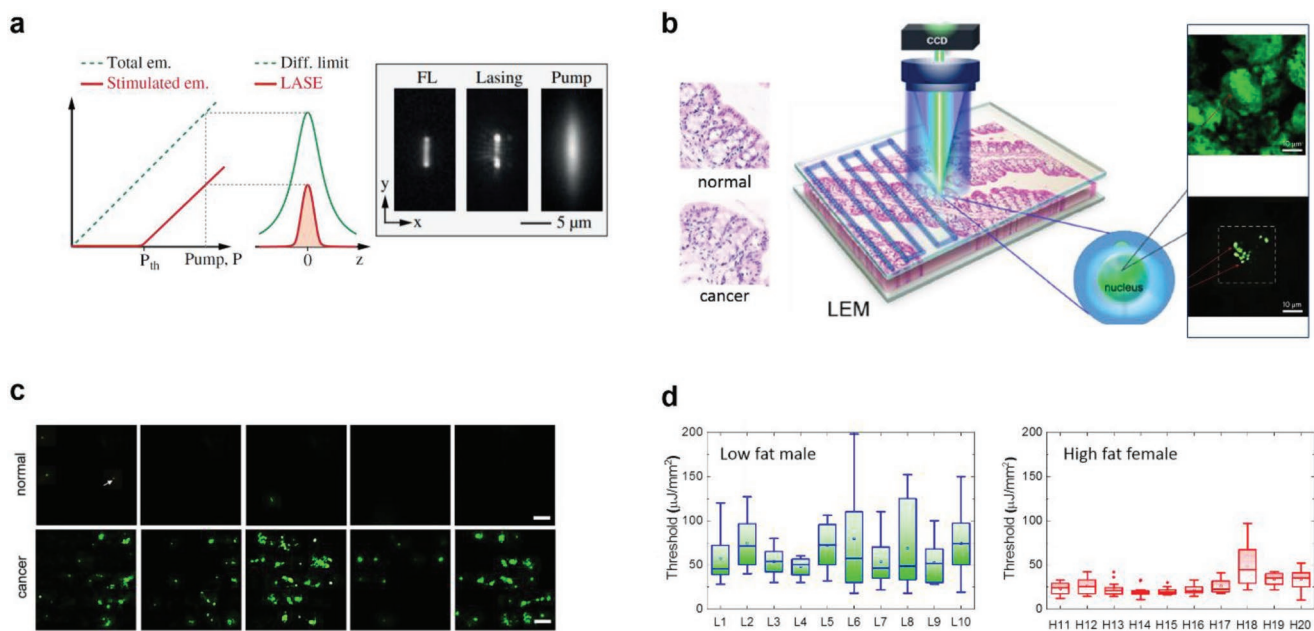


Figure 10. a) Principle of laser stimulated emission (LASE) microscopy. Left panel: The output energy from a laser particle as a function of pump intensity. The laser output increases steeply at pump energy above the threshold (P_{th}). Center panel: The point spread function (PSF) of laser emission (red line) in comparison to the traditional diffraction-limited PSF of fluorescence detection (green line). Both the resolution and signal-to-background contrast are enhanced in LASE microscopy. Right panel: Comparison of fluorescence emission, laser emission of the perovskite, and pump beam captured from CCD. Adapted with permission.^[13] Copyright 2017, American Physical Society. b) Conceptual illustration of laser emission microscopy (LEM) for cell and tissue mapping. The right inset shows the comparison of traditional fluorescence microscopy and LEM in a cell nucleus labeled with EGFR-FITC. Adapted with permission.^[43,48] Copyrights as in (c) and (d). c) Examples of LEM of a set of normal and cancer tissues. Cancer tissues have significantly more lasing spots than normal tissues. Adapted with permission.^[43] Copyright 2017, Springer Nature. d) Comparison of the lasing thresholds of low-fat fed male mice and high-fat fed female mice. Adapted with permission.^[48] Copyright 2019, Optical Society of America.

lasing particles have been used in cell tracking with massive multiplexicity, smaller (<100 nm) lasing particles would be even more interesting due to less stress on cells by those particles.

- 3) While for the tracking purposes, the lasing characteristics are required to maintain stable (so that each individual cells can be uniquely identified), the lasing characteristics need to be highly sensitive to any environmental changes (such as pH, temperature, local biomolecular concentration, and

local force/pressure, etc.) for intracellular sensing applications. As compared to fluorescence (such as that from dyes) and scattering (such as that from gold nanoparticles), lasing emission has orders of magnitude narrower linewidth, which results in significantly improved detection limit. In addition, lasing emission intensity is much more sensitive to environmental changes than fluorescence (due to optical feedback mechanism in lasing action), which can also be exploited for sensing. Unfortunately, the existing intracellular laser probes

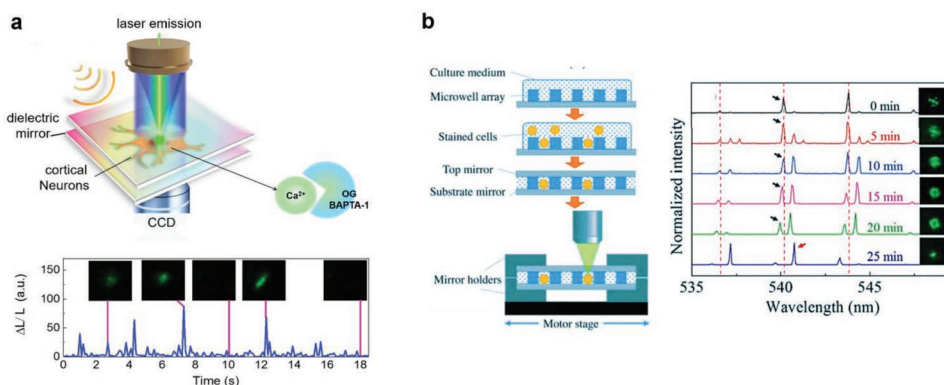


Figure 11. a) Top: Concept of optical recording of neuron spiking with a neuron laser, in which neurons are sandwiched inside an FP cavity. Bottom: Short-term laser recording of calcium transients caused by spontaneous neuronal activities over 18 s from a single neuron. The insets show the representative laser emission images captured by a CCD camera. Adapted with permission.^[101] Published under a CC-BY-NC-ND 4.0 International license, Copyright 2019, The Authors. b) Cell laser array. The cells are stained with dyes and placed inside an FP cavity. The lasing spectrum of each cell and the corresponding lasing mode profile can be monitored over time. Adapted with permission.^[31] Copyright 2017, Royal Society of Chemistry.

have micrometer or sub-micrometer dimensions, much larger than dyes and nanoparticles (such as quantum dots and gold nanoparticles). Therefore, it is critical to develop laser probes with a size below 100 nm.

- 4) Combination of biolasers with other modalities such as ultrasound and photoacoustic techniques will significantly expand the capability of detection and imaging. The laser particles can serve as the contrast agent. In turn other techniques such as ultrasound can help modulate and localize the laser particles to achieve a higher signal to noise ratio and better spatial resolution in deep tissue imaging.
- 5) Although not quite related to sensing and detection, biological materials can be excellent building blocks for the development of the laser itself. For example, many biomaterials, such as fluorescent proteins, chlorophyll, luciferin, and vitamin can be excellent gain media^[5,10,11,22,102,103] and can be synthesized at a large scale. In addition, biomaterials such as DNA, antibodies, enzymes have unique properties of self-recognition and self-assembly, which can be exploited to develop biocontrolled or bioconfigurable lasers.^[4,18,19,29]

Despite numerous technological advances made in the past decade, biolasers are still facing a few challenges, some of which are intrinsic to all biolasers and others may be related to a particular laser cavity, biomaterial, and application. Below we list a few that we hope to overcome by the future research and development.

- 1) While the lasing threshold behavior is advantageous in terms of enhancing the signal-to-noise ratio and signal-to-background ratio, a biolaser requires the external pump to be above its lasing threshold to conduct any meaningful measurement. Consequently, a high pump intensity is needed when the cavity has a relatively low Q -factor and the density or concentration of the gain medium is low (i.e., the gain is low), which may potentially result in damage to biological samples and require sophisticated and expensive equipment (such as expensive pulsed pump lasers instead of inexpensive CW lasers). Although in many cases, a single and a few excitation pulses are sufficient to acquire lasing signal with an acceptable signal-to-noise ratio, better cavity designs, and gain media may be needed to further lower the exposure of the biomolecules/cells to pumping light.
- 2) Since the laser light inside a cavity is bounced back and forth between two mirrors, the laser output represents an accumulative effect along the z -direction (i.e., the laser emission direction). As a result, during laser imaging we may lose information in the z -direction. Recovery of the information in the z -direction (i.e., performing z -sectioning) in the laser emission based imaging would be the next important step in the biolaser development.
- 3) Since for a given external pump, a biolaser requires the fluorophore to reach a certain concentration to overcome the threshold, the molecules and cells with low fluorophore concentrations may be missed, as they may be below the lasing threshold. How to enhance the dynamic range to recapture the molecules and cells (and the sites on a tissue when doing imaging) of low labeling concentration (or density) would be another challenging yet important topic.

Acknowledgements

The authors thank the support from National Science Foundation under ECCS-1607250.

Conflict of Interest

The authors declare no conflict of interest.

Keywords

bioimaging, biological lasers, biomedical sensing, labeling, mapping, microresonators, nanoresonators, tracking

Received: March 3, 2019

Revised: May 4, 2019

Published online: June 11, 2019

- [1] B. D. Guenther, B. Jopson, R. John Koshel, B. Paldus, *Opt. Photonics News* **2005**, 16, 14.
- [2] P. L. Gourley, *Nat. Med.* **1996**, 2, 942.
- [3] L. Wang, D. Liu, N. He, S. L. Jacques, S. L. Thomsen, *Appl. Opt.* **1996**, 35, 1775.
- [4] Y. Sun, S. I. Shopova, C.-S. Wu, S. Arnold, X. Fan, *Proc. Natl. Acad. Sci. USA* **2010**, 107, 16039.
- [5] M. C. Gather, S. H. Yun, *Nat. Photonics* **2011**, 5, 406.
- [6] X. Fan, S.-H. Yun, *Nat. Methods* **2014**, 11, 141.
- [7] P. L. Gourley, *J. Phys. D: Appl. Phys.* **2003**, 36, R228.
- [8] P. L. Gourley, J. K. Hendricks, A. E. McDonald, R. Copeland, K. E. Barrett, C. R. Gourley, R. K. Naviaux, *Biomed. Microdevices* **2005**, 7, 331.
- [9] X. Wu, M. K. K. Oo, K. Reddy, Q. Chen, Y. Sun, X. Fan, *Nat. Commun.* **2014**, 5, 3779.
- [10] X. Wu, Q. Chen, Y. Sun, X. Fan, *Appl. Phys. Lett.* **2013**, 102, 203706.
- [11] S. Nizamoglu, M. C. Gather, S. H. Yun, *Adv. Mater.* **2013**, 25, 5943.
- [12] A. H. Fikouras, M. Schubert, M. Karl, J. D. Kumar, S. J. Powis, A. Di Falco, M. C. Gather, *Nat. Commun.* **2018**, 9, 4817.
- [13] S. Cho, M. Humar, N. Martino, S. H. Yun, *Phys. Rev. Lett.* **2016**, 117, 193902.
- [14] X. Wu, Q. Chen, P. Xu, Y.-C. Chen, B. Wu, R. M. Coleman, L. Tong, X. Fan, *Nanoscale* **2018**, 10, 9729.
- [15] N. Martino, S. J. J. Kwok, A. C. Liapis, S. Forward, S.-J. Jang, S. H. Yun, in *CLEO*, San Jose, CA, May **2018**.
- [16] N. Martino, S. J. J. Kwok, A. C. Liapis, S. Forward, H. Jang, H. M. Kim, S. J. Wu, P. H. Dannenberg, S. J. Jang, Y. H. Lee, S. H. Yun, *bioRxiv*, 465104, **2018**; to be published in *Nat. Photon.* **2019**.
- [17] M. Song, H. Baek, G.-C. Yi, presented at CLEO, San Jose, CA, May **2019**.
- [18] X. Zhang, W. Lee, X. Fan, *Lab Chip* **2012**, 12, 3673.
- [19] Q. Chen, M. Ritt, S. Sivaramakrishnan, Y. Sun, X. Fan, *Lab Chip* **2014**, 14, 4590.
- [20] Q. Chen, X. Zhang, Y. Sun, M. Ritt, S. Sivaramakrishnan, X. Fan, *Lab Chip* **2013**, 13, 2679.
- [21] W. Lee, X. Fan, *Anal. Chem.* **2012**, 84, 9558.
- [22] Y.-C. Chen, Q. Chen, X. Fan, *Lab Chip* **2016**, 16, 2228.
- [23] U. Bog, T. Laue, T. Grossmann, T. Beck, T. Wienhold, B. Richter, M. Hirtz, H. Fuchs, H. Kalt, T. Mappes, *Lab Chip* **2013**, 13, 2701.
- [24] T. Baba, *MRS Commun.* **2015**, 5, 555.
- [25] G. McConnell, S. Mabbott, A. L. Kanibolotsky, P. J. Skabara, D. Graham, G. A. Burley, N. Laurand, *Langmuir* **2018**, 34, 14766.

- [26] M. Gao, C. Wei, X. Lin, Y. Liu, F. Hu, Y. S. Zhao, *Chem. Commun.* **2017**, 53, 3102.
- [27] M. Aas, Q. Chen, A. Jonas, A. Kiraz, X. Fan, *IEEE J. Sel. Top. Quantum Electron.* **2016**, 22, 188.
- [28] C. P. Dietrich, A. Steude, L. Tropic, M. Schubert, N. M. Kronenberg, K. Ostermann, S. Höfling, M. C. Gather, *Sci. Adv.* **2016**, 2, e1600666.
- [29] Q. Chen, H. Liu, W. Lee, Y. Sun, D. Zhu, H. Pei, C. Fan, X. Fan, *Lab Chip* **2013**, 13, 3351.
- [30] S. Nizamoglu, K.-B. Lee, M. C. Gather, K. S. Kim, M. Jeon, S. Kim, M. Humar, S.-H. Yun, *Adv. Opt. Mater.* **2015**, 3, 1197.
- [31] Q. Chen, Y.-C. Chen, Z. Zhang, B. Wu, R. Coleman, X. Fan, *Lab Chip* **2017**, 17, 2814.
- [32] P. L. Gourley, R. K. Naviaux, *IEEE J. Sel. Top. Quantum Electron.* **2005**, 11, 818.
- [33] A. JonÅiÅj, M. Aas, Y. Karadag, S. ManioÅyly, S. Anand, D. McGloin, H. Bayraktar, A. Kiraz, *Lab Chip* **2014**, 14, 3093.
- [34] Y.-C. Chen, Q. Chen, X. Fan, *Optica* **2016**, 3, 809.
- [35] R. C. Polson, Z. Vardeny, *Appl. Phys. Lett.* **2004**, 85, 1289.
- [36] Q. Song, S. Xiao, Z. Xu, J. Liu, X. Sun, V. Drachev, V. M. Shalaev, O. Akkus, Y. L. Kim, *Opt. Lett.* **2010**, 35, 1425.
- [37] Z. Lv, Z. Man, Z. Xu, C. Feng, Y. Yang, Q. Liao, X. Wang, L. Zheng, H. Fu, *ACS Appl. Mater. Interfaces* **2018**, 10, 32981.
- [38] E. I. Galanzha, R. Weingold, D. A. Nedosekin, M. Sarimollaoglu, J. Nolan, W. Harrington, A. S. Kuchyanov, R. G. Parkhomenko, F. Watanabe, Z. Nima, A. S. Biris, A. I. Plekhanov, M. I. Stockman, V. P. Zharov, *Nat. Commun.* **2017**, 8, 15528.
- [39] A. Fernandez-Bravo, K. Yao, E. S. Barnard, N. J. Borys, E. S. Levy, B. Tian, C. A. Tajon, L. Moretti, M. V. Altoe, S. Aloni, K. Beketayev, F. Scotognella, B. E. Cohen, E. M. Chan, P. J. Schuck, *Nat. Nanotechnol.* **2018**, 13, 572.
- [40] X. Li, Y. Qin, X. Tan, Y.-C. Chen, Q. Chen, W.-H. Weng, X. Wang, X. Fan, *ACS Photonics* **2019**, 6, 531.
- [41] M. Humar, A. Dobravec, X. Zhao, S. H. Yun, *Optica* **2017**, 4, 1080.
- [42] Y.-C. Chen, Q. Chen, T. Zhang, W. Wang, X. Fan, *Lab Chip* **2017**, 17, 538.
- [43] Y.-C. Chen, X. Tan, Q. Sun, Q. Chen, W. Wang, X. Fan, *Nat. Biomed. Eng.* **2017**, 1, 724.
- [44] Y.-C. Chen, Q. Chen, X. Wu, X. Tan, J. Wang, X. Fan, *Lab Chip* **2018**, 18, 1057.
- [45] M. Schubert, K. Volckaert, M. Karl, A. Morton, P. Liehm, G. B. Miles, S. J. Powis, M. C. Gather, *Sci. Rep.* **2017**, 7, 40877.
- [46] M. Schubert, A. Steude, P. Liehm, N. M. Kronenberg, M. Karl, E. C. Campbell, S. J. Powis, M. C. Gather, *Nano Lett.* **2015**, 15, 5647.
- [47] Lasers in Micro, Nano and Bio Systems - 2018, <https://www.grc.org/lasers-in-micro-nano-and-bio-systems-conference/2018/> (accessed: June 2019).
- [48] Y.-C. Chen, Q. Chen, X. Tan, G. Chen, I. Bergin, M. N. Aslam, X. Fan, *Biomed. Opt. Express* **2019**, 10, 838.
- [49] C. Feng, Z. Xu, X. Wang, H. Yang, L. Zheng, H. Fu, *ACS Appl. Mater. Interfaces* **2017**, 9, 7385.
- [50] W. Wang, C. Zhou, T. Zhang, J. Chen, S. Liu, X. Fan, *Lab Chip* **2015**, 15, 3862.
- [51] M. Humar, M. C. Gather, S.-H. Yun, *Opt. Express* **2015**, 23, 27865.
- [52] X. Wu, Y. Wang, Q. Chen, Y.-C. Chen, X. Li, L. Tong, X. Fan, *Photonics Res.* **2019**, 7, 50.
- [53] C. Gong, Y. Gong, M. K. Khaing Oo, Y. Wu, Y. Rao, X. Tan, X. Fan, *Biosens. Bioelectron.* **2017**, 96, 351.
- [54] X. Yang, W. Shu, Y. Wang, Y. Gong, C. Gong, Q. Chen, X. Tan, G. D. Peng, X. Fan, Y. J. Rao, *Biosens. Bioelectron.* **2019**, 131, 60.
- [55] M. Hou, X. Liang, T. Zhang, C. Qiu, J. Chen, S. Liu, W. Wang, X. Fan, *ACS Sens.* **2018**, 3, 1750.
- [56] J. A. Rivera, J. Eden, *Opt. Express* **2016**, 24, 10858.
- [57] W. Lee, Q. Chen, X. Fan, D. K. Yoon, *Lab Chip* **2016**, 16, 4770.
- [58] V. D. Ta, S. Caixeiro, F. M. Fernandes, R. Sapienza, *Adv. Opt. Mater.* **2017**, 5, 1601022.
- [59] V. D. Ta, R. Chen, H. D. Sun, *Sci. Rep.* **2013**, 3, 1362.
- [60] G. Aubry, Q. Kou, J. Soto-Velasco, C. Wang, S. Meance, J. J. He, A. M. Haghiri-Gosnet, *Appl. Phys. Lett.* **2011**, 98, 111111.
- [61] T. J. Kippenberg, J. Kalkman, A. Polman, K. J. Vahala, *Phys. Rev. A* **2006**, 74, 051802.
- [62] Y. Yang, A. Q. Liu, L. Lei, L. K. Chin, C. D. Ohl, Q. J. Wang, H. S. Yoon, *Lab Chip* **2011**, 11, 3182.
- [63] H. Chandralalim, Q. Chen, A. A. Said, M. Dugan, X. Fan, *Lab Chip* **2015**, 15, 2335.
- [64] C. Gong, Y. Gong, Q. Chen, Y.-J. Rao, G.-D. Peng, X. Fan, *Lab Chip* **2017**, 17, 3431.
- [65] C. Gong, Y. Gong, X. Zhao, Y. Luo, Q. Chen, X. Tan, Y. Wu, X. Fan, G.-D. Peng, Y.-J. Rao, *Lab Chip* **2018**, 18, 2741.
- [66] Y. Xu, C. Gong, Q. Chen, Y. Luo, Y. Wu, Y. Wang, G. D. Peng, Y. J. Rao, X. Fan, Y. Gong, *IEEE J. Sel. Top. Quantum Electron.* **2019**, 25, 1.
- [67] Z. Gao, W. Zhang, Y. Yan, J. Yi, H. Dong, K. Wang, J. Yao, Y. S. Zhao, *ACS Nano* **2018**, 12, 5734.
- [68] Y. Wei, X. Lin, C. Wei, W. Zhang, Y. Yan, Y. S. Zhao, *ACS Nano* **2017**, 11, 597.
- [69] S. S. Lee, J. B. Kim, Y. H. Kim, S.-H. Kim, *Sci. Adv.* **2018**, 4, eaat8276.
- [70] Y. Wang, L. Zhao, A. Xu, L. Wang, L. Zhang, S. Liu, Y. Liu, H. Li, *Sens. Actuators, B* **2018**, 258, 1090.
- [71] M. Humar, *Liq. Cryst.* **2016**, 43, 1937.
- [72] L. Zhao, Y. Wang, Y. Yuan, Y. Liu, S. Liu, W. Sun, J. Yang, H. Li, *Opt. Commun.* **2017**, 402, 181.
- [73] T. Kumar, M. A. Mohiddon, N. Dutta, N. K. Viswanathan, S. Dhara, *Appl. Phys. Lett.* **2015**, 106, 051101.
- [74] S. Kita, K. Nozaki, S. Hachuda, H. Watanabe, Y. Saito, S. Otsuka, T. Nakada, Y. Arita, T. Baba, *IEEE J. Sel. Top. Quantum Electron.* **2011**, 17, 1632.
- [75] S. Hachuda, S. Otsuka, S. Kita, T. Isono, M. Narimatsu, K. Watanabe, Y. Goshima, T. Baba, *Opt. Express* **2013**, 21, 12815.
- [76] T. Isono, S. Hachuda, K. Watanabe, N. Yamashita, Y. Goshima, T. Baba, presented at Tech. Dig. MRS Annual Meet., Boston, MA, December **2013**.
- [77] K. Watanabe, M. Nomoto, F. Nakamura, S. Hachuda, A. Sakata, T. Watanabe, Y. Goshima, T. Baba, *Biosens. Bioelectron.* **2018**, 117, 161.
- [78] T. Watanabe, Y. Saijo, Y. Hasegawa, K. Watanabe, Y. Nishijima, T. Baba, *Opt. Express* **2017**, 25, 24469.
- [79] Z. Li, Z. Zhang, A. Scherer, D. Psaltis, *Opt. Express* **2006**, 14, 10494.
- [80] Z. Li, D. Psaltis, *IEEE J. Sel. Top. Quantum Electron.* **2007**, 13, 185.
- [81] C. Vannahme, F. Maier-Flaig, U. Lemmer, A. Kristensen, *Lab Chip* **2013**, 13, 2675.
- [82] M. Karl, J. M. E. Glackin, M. Schubert, N. M. Kronenberg, G. A. Turnbull, I. D. W. Samuel, M. C. Gather, *Nat. Commun.* **2018**, 9, 1525.
- [83] M. Lu, S. S. Choi, U. Irfan, B. T. Cunningham, *Appl. Phys. Lett.* **2008**, 93, 111113.
- [84] A. Retolaza, J. Martinez-Perdiguero, S. Merino, M. Morales-Vidal, P. G. Boj, J. A. Quintana, J. M. Villalvilla, M. A. Díaz-García, *Sens. Actuators, B* **2016**, 223, 261.
- [85] X. Liu, T. Li, T. Yi, C. Wang, J. Li, M. Xu, D. Huang, S. Liu, S. Jiang, Y. Ding, *J. Mod. Opt.* **2016**, 63, 1248.
- [86] J. Ziegler, M. Djiango, C. Vidal, C. Hrelescu, T. A. Klar, *Opt. Express* **2015**, 23, 15152.
- [87] M. Gaio, S. Caixeiro, B. Marelli, F. G. Omenetto, R. Sapienza, *Phys. Rev. Appl.* **2017**, 7, 034005.
- [88] E. Ignesti, F. Tommasi, L. Fini, F. Martelli, N. Azzali, S. Cavalieri, *Sci. Rep.* **2016**, 6, 37113.
- [89] S. Caixeiro, M. Gaio, B. Marelli, F. G. Omenetto, R. Sapienza, *Adv. Opt. Mater.* **2016**, 4, 998.
- [90] W. Z. Wan Ismail, G. Liu, K. Zhang, E. M. Goldys, J. M. Dawes, *Opt. Express* **2016**, 24, A85.

- [91] R. C. Polson, Z. V. Vardeny, *J. Opt.* **2010**, *12*, 024010.
- [92] F. Lahoz, I. R. Martín, M. Urgellés, J. Marrero-Alonso, R. Marín, C. J. Saavedra, A. Boto, M. Díaz, *Laser Phys. Lett.* **2015**, *12*, 045805.
- [93] Y. Wang, Z. Duan, Z. Qiu, P. Zhang, J. Wu, D. Zhang, T. Xiang, *Sci. Rep.* **2017**, *7*, 8385.
- [94] L. M. G. Abegão, A. A. C. Pagani, S. C. Zílio, M. A. R. C. Alencar, J. J. Rodrigues, *Sci. Rep.* **2016**, *6*, 35119.
- [95] R. F. Oulton, V. J. Sorger, T. Zentgraf, R.-M. Ma, C. Gladden, L. Dai, G. Bartal, X. Zhang, *Nature* **2009**, *461*, 629.
- [96] M. A. Noginov, G. Zhu, A. M. Belgrave, R. Bakker, V. M. Shalaev, E. E. Narimanov, S. Stout, E. Herz, T. Suteewong, U. Wiesner, *Nature* **2009**, *460*, 1110.
- [97] R.-M. Ma, S. Ota, Y. Li, S. Yang, X. Zhang, *Nat. Nanotechnol.* **2014**, *9*, 600.
- [98] A. Yang, T. B. Hoang, M. Dridi, C. Deeb, M. H. Mikkelsen, G. C. Schatz, T. W. Odom, *Nat. Commun.* **2015**, *6*, 6939.
- [99] M. Humar, S. Hyun Yun, *Nat. Photonics* **2015**, *9*, 572.
- [100] M. Schubert, L. Woolfson, I. R. M. Barnard, A. Morton, B. Casement, G. B. Robertson, G. B. Miles, S. J. Pitt, C. S. Tucker, M. C. Gather, bioRxiv, 605444, **2019**.
- [101] Y.-C. Chen, X. Li, H. Zhu, W.-H. Weng, X. Tan, Q. Chen, X. Wang, X. Fan, bioRxiv, 584938, **2019**.
- [102] M. C. Gather, S. H. Yun, *Nat. Commun.* **2014**, *5*, 5722.
- [103] X. Zhang, Q. Chen, M. Ritt, S. Sivaramakrishnan, X. Fan, *Proc. SPIE* **2013**, *8629*, 862907.